JACS
JOURNAL OF THE AMERICAN CHEMICAL SOCIETY
Article
pubs.acs.org/JACS

Steady-State Catalytic Wave-Shapes for 2-Electron Reversible Electrocatalysts and Enzymes

Vincent Fourmond,[†] Carole Baffert,[†] Kateryna Sybirna,[‡] Thomas Lautier,[§] Abbas Abou Hamdan,[†] Sébastien Dementin,[†] Philippe Soucaille,[§] Isabelle Meynial-Salles,[§] Hervé Bottin,[‡] and Christophe Léger[†,*]

[†]CNRS, Aix-Marseille Univ, BIP UMR 7281, IMM FR 3479, 31 chemin J. Aiguier, 13402 Marseille Cedex 20, France

[‡]iBiTec-S SB2SM, LMB (UMR CNRS 8221), DSV, CEA, 91191 Gif-sur-Yvette, France

[§]Université de Toulouse, INSA, UPS, INP, LISBP, INRA:UMR792, CNRS:UMR 5504, 135 Avenue de Rangueil, 31077 Toulouse, France

Supporting Information

ABSTRACT: Using direct electrochemistry to learn about the mechanism of electrocatalysts and redox enzymes requires that kinetic models be developed. Here we thoroughly discuss the interpretation of electrochemical signals obtained with adsorbed enzymes and molecular catalysts that can reversibly convert their substrate and product. We derive analytical relations between electrochemical observables (overpotentials for catalysis in each direction, positions, and magnitudes of the features of the catalytic wave) and the characteristics of the catalytic cycle (redox properties of the catalytic intermediates, kinetics of intramolecular and interfacial electron transfer, etc.). We discuss whether or not the position of the wave is determined by the redox potential of a redox relay when intramolecular electron transfer is slow. We demonstrate that there is no simple relation between the reduction potential of the active site and the catalytic bias of the enzyme, defined as the ratio of the oxidative and reductive limiting currents; this explains the recent experimental observation that the catalytic bias of NiFe hydrogenase depends on steps of the catalytic cycle that occur far from the active site [Abou Hamdan et al., *J. Am. Chem. Soc.* **2012**, *134*, 8368]. On the experimental side, we examine which models can best describe original data obtained with various NiFe and FeFe hydrogenases, and we illustrate how the presence of an intramolecular electron transfer chain affects the voltammetry by comparing the data obtained with the FeFe hydrogenases from *Chlamydomonas reinhardtii* and *Clostridium acetobutylicum*, only one of which has a chain of redox relays. The considerations herein will help the interpretation of electrochemical data previously obtained with various other bidirectional oxidoreductases, and, possibly, synthetic inorganic catalysts.

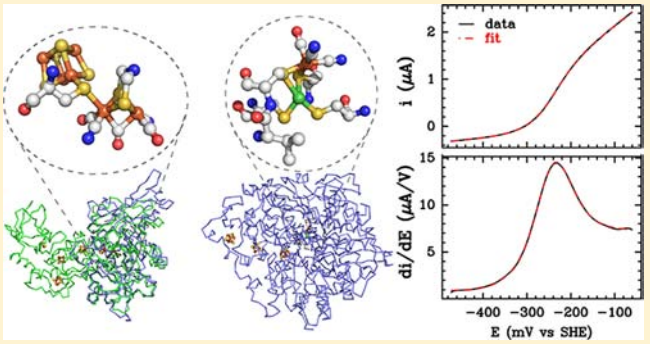

INTRODUCTION

Nearly 30 years have passed since it was first demonstrated that enzymes can be adsorbed onto electrodes in a configuration that allows direct electron transfer (ET) and retention of the enzyme's native properties.[1−3] Direct ET has since been achieved with enzymes that catalyze various reactions, using organic (flavin, PQQ) or inorganic (nickel-, iron- or copper-containing) cofactors. This configuration proved very useful in the context of mechanistic studies of redox enzymes.[4] Indeed, the catalytic current is simply proportional to the enzyme's turnover rate, and this electrochemical measurement of activity has two fundamental advantages over the more traditional kinetic methods based on solution assays. First, the enzyme's activity can be sampled at a very high frequency, which is important for measuring the rates and learning about the mechanisms of inhibition[5] or (in)activation.[6−8] Second, the steady-state activity can be measured as a function of the electrode potential, whose value sets (albeit indirectly) the redox state of the enzyme. Measuring the activity in the potential domain sometimes makes it possible to determine the reduction potential of the catalytic intermediates, to detect chemical reactions that are coupled to their redox transformations,[9] or to learn about electron-transfer steps which occur at a distance from the active site. In many respiratory enzymes, a chain of redox centers "wires" the site where the chemistry occurs to the site where the redox partner gives or receives electrons,[10,11] and studying the kinetics of long-range, intramolecular ET using electrochemistry is of particular interest.

Voltammetry is ideal for probing both reductive and oxidative catalysis in a single experiment where the electrode potential is swept over a large range. In the presence of both the substrate and the product of the reaction, the catalytic

Received: November 27, 2012
Published: January 30, 2013

dx.doi.org/10.1021/ja311607s | *J. Am. Chem. Soc.* 2013, 135, 3926−3938

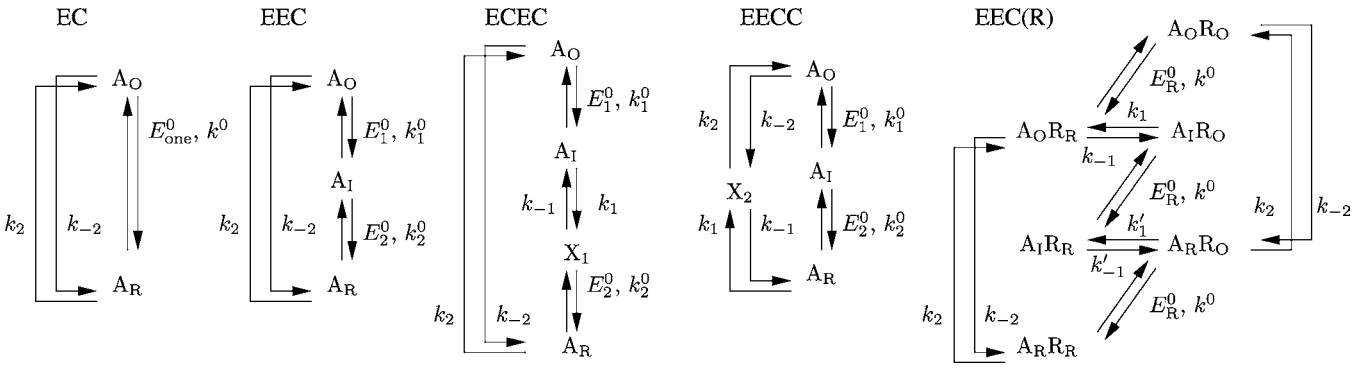

Figure 1. The five kinetic schemes considered in this paper, and referred to according to the electrochemical terminology, from the simplest one-electron EC model, to the most complex EEC(R) scheme, which takes into account the one-electron relay that mediates ET from the two-electron active site to the electrode. The redox state of the active site is depicted by the letter A with a subscript O (for "oxidized"), I (intermediate), or R (reduced). In the rightmost scheme, "R" is the relay that can be either oxidized or reduced. X_1 and X_2 are catalytic intermediates.

current tends to high- and low-potential limiting values whose ratio reveals the "catalytic bias" of the enzyme, that is, its preference for catalyzing the reaction in one particular direction. Using voltammetry, it cannot be missed that certain redox enzymes are able to catalyze substrate/product conversion in both directions, whereas others only work one way. Thermodynamics imposes that the rate be zero when the electrode potential equates to the reduction potential of the substrate/product couple,[9,12−14] but the electrochemical response on either side of the open circuit potential (OCP) is entirely defined by the properties of the enzyme. The question of what are the molecular and kinetic determinants of catalytic reversibility has seldom been addressed. Regarding oxidoreductases, an interesting, open debate regards whether or not the catalytic bias, defined as the ratio of maximal rates in the two directions of the reaction, is imposed by the redox properties of the centers in the enzyme (refs 14, 15 and refs therein). Whether a particular enzyme is a better catalyst of oxidation or reduction is indeed often discussed by comparing the potential of the substrate/product redox couple with the potential of either the active site or the electron transfer (ET) chain, but a genuine relation of cause and effect has never been established (ref 14 and refs therein). In contrast, we recently studied a number of NiFe hydrogenase mutants (hydrogenases are enzymes that reversibly converts dihydrogen and protons according to $H_2 \rightleftharpoons 2H^+ + 2e^-$), and we have observed that mutations of amino acids that are remote from the active site, and have no effect on the redox properties of the active site, may strongly alter the enzyme's catalytic bias.[14,16] In contrast to hydrogenases, many bioinspired catalysts appear to work only one way. In the case of the reaction of H_2 formation and oxidation, which has been the subject of a very large number of investigations, it is indeed striking that there are many synthetic catalysts of H_2 evolution and far fewer molecular complexes that perform H_2 oxidation. The latter will be needed for developing a H_2 based economy,[17,18] and understanding what makes certain biological catalysts more efficient in one particular direction of the reaction may eventually help bridge the gap between biological and inorganic catalysis.

Gaining any useful information from the voltammetric signals of adsorbed enzymes requires that appropriate kinetic models be available. The wave-shapes are still often characterized by measuring (1) the midpoint potentials of the catalytic waves, (2) an apparent number of electrons, which define the steepness of the waves, and (3) limiting currents in each direction.[19] The interpretation of these empirical parameters is only possible if they can be related to meaningful kinetic parameters. In this context, recent results in our group include the modeling of voltammetric signals that strongly depart from steady-state and/or exhibit several inflections and extrema.[7,20] All published models but one[15] have considered the case were the enzyme catalyzes the reaction in only one direction; neglecting the backward reaction is correct if the enzyme is only able to work forward or if the concentration of the substrate of the backward reaction is maintained close to zero by using a rotating disc electrode. The authors of ref 15 described *two-electron* catalysis by hydrogenase using an electrochemical rate equation derived from a *one-electron*, reversible catalytic cycle, suggesting that this may be a good approximation when intramolecular ET is rate limiting (we shall discuss the validity of this assumption).

Here, we discuss the relevance of several models that can be used for interpreting the steady-state voltammograms obtained for two-electron, reversible electrocatalysts under conditions of direct electron transfer. The models take into account both interfacial and intramolecular electron transfer. We examine which wave-shapes can be obtained, and we explain how the positions of their features inform on steps which are part of the catalytic cycle, such as chemical reactions coupled to the redox transformations of the active site, or long-range intramolecular electron transfer. We demonstrate that there is no simple relation (in the most general case) between the redox properties of the active site and the catalytic bias (defined herein as the ratio of the limiting currents in the two directions). We examine the relation between catalytic bias and overpotentials in each direction, which is relevant to the design and optimization of synthetic catalysts.[21] We show that the models accurately describe the catalytic signals obtained with the FeFe hydrogenases from *Chlamydomonas reinhardtii* and *Clostridium acetobutylicum*. The former has a single cofactor, the active site "H-cluster",[22] whereas the latter has a chain of redox cofactors that mediate long-range electron transfer to and from the active site;[23,24] we show that this difference in cofactor composition is in complete agreement with the analysis of the wave-shapes; in other words, we can detect the presence of the relay from the shape of the catalytic signal.

dx.doi.org/10.1021/ja311607s | J. Am. Chem. Soc. 2013, 135, 3926−3938

RESULTS AND DISCUSSION

The Models and the Basic Hypotheses. Figure 1 shows catalytic cycles from which we shall derive rate equations. The redox state of the active site of the immobilized enzyme is depicted by the letter A with a subscript O (for "oxidized"), I (intermediate), or R (reduced) (the notations are the same as in ref 25). The schemes are referred to by the names EC, EEC, etc. according to the electrochemical terminology. The letter E refers to a one-electron redox step, whereby the active site of the enzyme is oxidized or reduced. The cycles include one or two redox transformations of the active site depending on the stoichiometry of the reaction that is catalyzed by the enzyme. The letters C indicate reversible chemical steps.

We do not consider substrate/product mass transport to and from the electrode where the enzyme is adsorbed, and we assume that the concentrations of substrate/product/protons are the same near the electrode surface and in the bulk of the electrochemical cell. This is a reasonable approximation if the enzyme is adsorbed onto a rotating electrode which is spun at a very high rate. References 26 and 27 describe the effect of substrate depletion near the electrode surface in the steady-state (at low electrode rotation rate). The price to pay for taking into account mass transport is that closed-form expression of the current cannot be obtained, in contrast to the situations examined below.

In the case of the EC, EEC, EECC, and ECEC models, we assume that electrons are directly transferred from the electrode to the active site. In many enzymes, however, the active site is buried in the protein, and "wired" to the protein surface by either one redox center[28] or a chain of redox centers.[10] We shall examine the effect of intramolecular ET on the reversible wave-shapes by considering the EEC(R) model, where interfacial ET changes the redox state of a relay, indicated by the letter R in the rightmost scheme of Figure 1; the steps whose rates are $k_{\pm 1}$ and $k'_{\pm 1}$ correspond to intramolecular ET between the active site and the relay; the rates $k_{\pm 2}$ of the chemical step are the same irrespective of the redox state of the relay (by assumption).

Each interfacial ET step is characterized by a reduction potential, E^0, and a rate of interfacial ET, k^0; we shall assume that the rates of oxidation or reduction of the active site or the relay obey Butler–Volmer kinetics,[29] with all transfer coefficients equal to $^1/_2$:

$$k_{\mathrm{ox/red}} = k^0 \exp\left(\pm \frac{f}{2}(E - E^0) \right) \tag{1}$$

The situation where interfacial ET is very fast on the time scale of turnover will be referred to as the Nernstian limit. Later in this paper we shall consider the case where the values of k^0 are not the same for all enzyme molecules, as occurs when their orientation on the electrode is not homogeneous.[30] We shall assume that all other parameters (reduction potentials and rate constants other than k^0) take the same values for all adsorbed enzyme molecules.

Each redox step might be coupled to reversible chemical reactions (not depicted in Figure 1), which are supposed to be very fast on the time scale of turnover, and therefore at equilibrium. This may include (de)protonations and/or the binding and release of the substrate/product. Such fast coupled reactions affect the apparent values of the reduction potentials and the apparent rates of interfacial ET.[31]

Importantly, that substrate binding may affect the reduction potential of the active site[31] means that the values of E^0 which appear in all equations hereafter may be different from the reduction potential of the catalyst determined in the absence of substrate.

The catalytic cycles in Figure 1 are closed by reversible chemical reactions (C), whose first-order (or pseudo-first-order) rates $k_{\pm 1}$ and $k_{\pm 2}$ are allowed to be slow on the time scale of turnover. For these reactions, positive subscripts correspond to the catalytic cycle turning in the direction that reduces the substrate (e.g., H_2 evolution in the case of hydrogenases). The pH and substrate/product concentrations are not explicitly considered, but, of course, they may affect the parameters of the model.

Notations. In the EC scheme (leftmost in Figure 1), the reduction potential of the active site has a subscript "one" to emphasize that it is that of a one-electron redox couple. For the two-electron cycles, E_1^0 and E_2^0 are the two one-electron reduction potentials of the active site, and E_0^0 is the average two-electron reduction potential $[E_0^0 = (E_1^0 + E_2^0)/2]$.

We shall use the compact notation $e_X = \exp[f(E - E_X^0)]$ with "X" substituted for "one", 1, 2 or 0; E is the electrode potential and $f = F/(RT)$. Therefore, $e_0 = (e_1 e_2)^{1/2}$. The parameter δ defines the difference between the one-electron potentials: $\delta = \exp[f/2(E_1^0 - E_2^0)] = (e_2/e_1)^{1/2}$, so that $e_1 = e_0/\delta$ and $e_2 = e_0\delta$. The greater δ, the more stable the half-reduced form of the active site.

We list and define all symbols in the Supporting Information section S10.

The Waves in the Nernstian Limit. Our goal here is to relate the values of the limiting currents and wave potentials to the rate constants and reduction potentials defined in Figure 1, in order to understand the physical meaning of the phenomenological parameters which characterize the position and shape of the wave. Useful information can be gained from the current equation calculated in the "Nernstian limit" where the rates of interfacial ET are much faster than the turnover rate. Indeed, sluggish interfacial ET may broaden the catalytic waves without changing the position of its main features (Figure 2).

In the Nernstian limit, all five models depicted in Figure 1 give steady-state current equations in the form

$$i = -\frac{nF\mathcal{A}\Gamma k_{\mathrm{R}}(1 - a')}{a} \tag{2}$$

where n is the number of electrons needed to turnover once, $\mathcal{A}$ is the electrode surface, Γ is the enzyme electroactive coverage, k_{R}, a', and a are nondimensional functions of the parameters of the model, which are made explicit in Supporting Information, Table S1. The functions a and a' contain terms with integer powers of e_n, and thus depend on the electrode potential; a and a' tend to 1 and 0, respectively, at low potential, where the current tends to the limiting value $i_{\mathrm{lim}}^{\mathrm{red}} = -nFA\Gamma k_{\mathrm{R}}$.

We first examine the two-electron models. In the Nernstian limit, each of them gives a current equation in the form

$$i = -\frac{2F\mathcal{A}\Gamma k_{\mathrm{R}}(1 - Ke_0^{\,2})}{1 + (\alpha\delta + \alpha'/\delta)e_0 + \beta e_0^{\,2}} \tag{3}$$

The relations between k_{R}, K, α, α', β, and the rate constants of the four models are given in Table 1.

To describe the position of the wave, two definitions of "catalytic potentials" can be used: (1) the positions of the

dx.doi.org/10.1021/ja311607s | J. Am. Chem. Soc. 2013, 135, 3926−3938

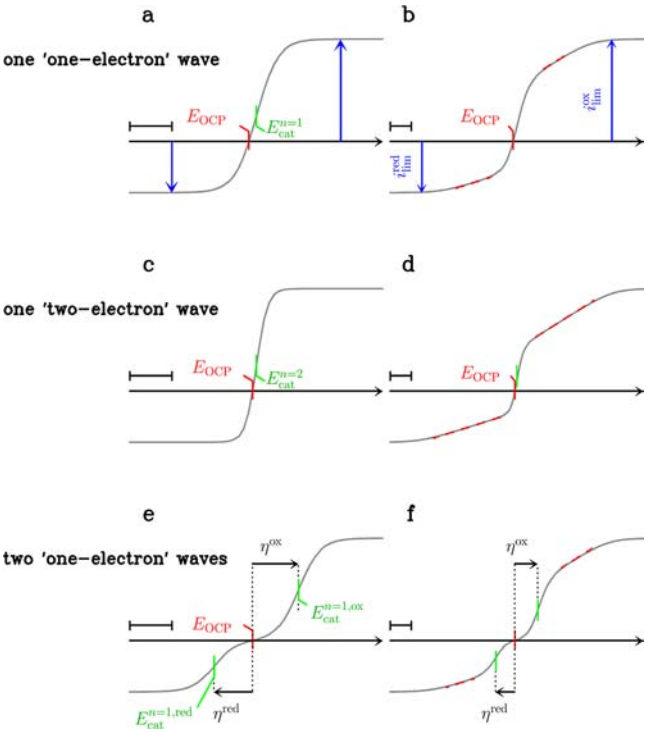

Figure 2. The typology of steady-state reversible catalytic waves predicted by the EC (top row) and the two-electron models (middle and bottom), in the Nernstian limit (left column), or when interfacial ET transfer is not infinitely fast (right column). These current/potential traces were calculated with eq 22 and Supporting Information, Table S1. In all panels, the horizontal segment is 100 mV long. The overpotential, defined as the difference between the catalytic potentials and the OCP, are indicated in panels e and f. Regarding panels c and d, there is essentially no overpotential since catalysis proceeds at a significant rate in either direction when the electrode potential is different from the OCP.

inflection points (the maxima of di/dE) or (2) the "mid-point" (or "half-wave") potentials where the current is the average of the plateau values on either side. If one is concerned with analyzing real data, we expect that there should be no significant difference between the two. In contrast, regarding the discussion of eq 3, the first definition gives extremely complex equations, and only the second definition is useful, and used hereafter.

The wave is a "two-electron sigmoid" (as illustrated in Figure 2c) if the term that is proportional to e_0^2 is larger than the term proportional to e_0, that is, if the following condition applies:

$$K_{disp} = \frac{\beta}{(\alpha\delta + \alpha'/\delta)^2} \gg 1 \tag{4}$$

where K_{disp} is the apparent disproportionation constant of the half reduced state of the active site. It is referred to as "apparent" because it depends on the rate constants in the catalytic cycle, rather than only on the two reduction potentials of the active site. In Supporting Information, section S2, we show that the midpoint potential of the two-electron sigmoid (referred to as a "two-electron catalytic potential," $E_{cat}^{n=2}$) is related to the reduction potential of the active site and the kinetic constants of the model by

$$E_{cat}^{n=2} = E_0^0 - \frac{1}{2f}\ln\beta \tag{5}$$

If the condition given by eq 4 is false, then the wave consists of a $n = 1$ oxidative wave and a $n = 1$ reductive wave, as illustrated in Figure 2e, whose midpoint potentials (referred to as "one-electron catalytic potentials") are

$$E_{cat}^{n=1,ox} = E_0^0 + \frac{1}{f}\ln\frac{\alpha\delta + \alpha'/\delta}{\beta} \tag{6a}$$

$$E_{cat}^{n=1,red} = E_0^0 - \frac{1}{f}\ln(\alpha\delta + \alpha'/\delta) \tag{6b}$$

respectively (cf. Supporting Information, section S2). It will be useful to keep in mind that $E_1^0 = E_0^0 + {}^1/_f \ln\delta$, $E_2^0 = E_0^0 - {}^1/_f \ln\delta$, and that

$$E_{cat}^{n=2} = (E_{cat}^{n=1,red} + E_{cat}^{n=1,ox})/2 \tag{7}$$

At low and high potentials, the current reaches limiting values

$$i_{lim}^{red} = -2F\mathcal{A}\Gamma k_R \tag{8a}$$

$$i_{lim}^{ox} = 2F\mathcal{A}\Gamma k_O \tag{8b}$$

respectively, with

Table 1. The Relations, For Each 2-Electron Catalytic Cycle in Figure 1, between the Parameters Defined in eq 3 and the Kinetic Constants of the Model

Model	k_R	K	α'	α	$\beta = Kk_R/k_O$
EEC	k_2	$\frac{k_{-2}}{k_2}$	0	1	1
EECC	$\frac{k_1 k_2}{k_1+k_2+k_{-1}}$	$\frac{k_{-1}k_{-2}}{k_1 k_2}$	0	$\frac{k_2+k_{-1}}{k_1+k_2+k_{-1}}$	$\frac{k_2+k_{-1}+k_{-2}}{k_1+k_2+k_{-1}}$
ECEC	$\frac{k_1 k_2}{k_1+k_2}$	$\frac{k_{-1}k_{-2}}{k_1 k_2}$	$\frac{k_2+k_{-2}}{k_1+k_2}$	$\frac{k_1+k_{-1}}{k_1+k_2}$	$\frac{k_{-1}+k_{-2}}{k_1+k_2}$
EEC(R)	$\frac{k_2 k_{-1} k'_{-1}}{k_{-1}(k_2+k'_{-1})+k'_{-1}(k_2+k_{-2})}$	$\frac{k_{-2}}{k_2}$	0	$\frac{k_2(k_1+k_{-1}+k'_{-1})+k_{-2}(k'_1+k'_{-1}+k_1)+k_{-1}k'_1}{k_{-1}(k_2+k'_{-1})+k'_{-1}(k_2+k_{-2})} \times \frac{k'_{-1}}{k'_1}$	$\frac{k_1(k_{-2}+k_2)+k'_1(k_1+k_{-2})}{k_{-1}(k_2+k'_{-1})+k'_{-1}(k_2+k_{-2})} \times \frac{k_{-1}k'_{-1}}{k_1 k'_1}$

dx.doi.org/10.1021/ja311607s | J. Am. Chem. Soc. 2013, 135, 3926−3938

$$k_O = Kk_R/\beta \quad (9)$$

From eq 3, we deduce that the OCP corresponds to $Ke_0^2 = 1$; that is

$$E_{OCP} = E_{cat}^{n=2} + \frac{1}{2f}\ln\frac{k_R}{k_O} \quad (10a)$$

$$= E_0^0 - \frac{1}{2f}\ln K \quad (10b)$$

The ratio k_R/k_O is a measure of the catalytic bias of the enzyme. The parameter K is an equilibrium constant that is distinct from the bias unless $\beta = 1$.

The Reduction Potential of the Active Site Is Not the Only Determinant of the Catalytic Bias. Equation 10a shows that there is a simple relation between the OCP, the bias ($-i_{lim}^{ox}/i_{lim}^{red} = k_O/k_R$), and depending on the shape of the waves, either the midpoint potential of the two-electron wave ($E_{cat}^{n=2}$) or the average of the midpoint potentials of the two one-electron waves. However, these catalytic potentials are convoluted parameters with no simple meaning. All models but the simplest EEC model predict that the catalytic potentials do not equate to the reduction potentials of the active site (cf. eqs 5−6, and Table 1). Therefore, *only* in the framework of the EEC model do the thermodynamic properties of the active site alone determine the catalytic bias.

The EEC model depicted in Figure 1 is realistic (and therefore the active site reduction potential defines the bias) only on condition that the catalytic cycle can be described as two half-cycles: one consisting of two redox steps coupled to chemical reactions that are very fast on the time scale of turnover, the other consisting of a chemical transformation that follows pseudo-first-order kinetics in both directions and entirely defines the ratio of maximal rates (that is, this reaction is rate-limiting under both very oxidizing and very reducing conditions). It is not clear to us how the corresponding experimental cases can be identified, but it is safe to assume that this will not correspond to a general situation, and that in many cases, the catalytic bias will not be imposed by the reduction potential of the active site. That the EEC mechanism is not appropriate for NiFe hydrogenases is supported by our recent findings that in various NiFe hydrogenase mutants, two *distinct* steps limit the maximal rates of H_2 oxidation and H_2 production; these steps are intermolecular ET and H_2-diffusion along the substrate channel, respectively. Certain mutations that have no effect on the redox properties of the active site slow only one of these steps, and selectively decrease one of the two maximal rates.[5,14,16,35]

We shall illustrate hereafter the link between catalytic bias and catalytic potential when we discuss the voltammetric data obtained with NiFe hydrogenase mutants (Figure 6).

The Meaning of the Catalytic Potentials When the Active Site Is *Directly* Oxidized or Reduced, or When All ET Steps Are Fast. The comparison of the EEC, ECEC, and EECC models sheds light on the meaning of the catalytic potentials when it is assumed that ET to/from the active site is direct. Equations 5−6 and the definitions in Table 1 of the kinetic parameters α, α', and β, clearly demonstrate that, unless the EEC model is valid (and thus $\alpha' = 0$, $\alpha = \beta = 1$), the midpoint potentials of the waves do not depend only on E_1^0 and E_2^0 and cannot be interpreted as thermodynamic parameters. The extent to which the catalytic potentials depart from the values of E^0 depends on the values of α, α', and β. Moreover, the values of E^0 may be affected by substrate binding, and may therefore be different from the potential of the catalyst measured in the absence of substrate.[31]

How the kinetics of *intramolecular* ET affects the magnitude, shape, and position of the catalytic wave can be understood by comparing the predictions of the EEC and EEC(R) models. If intramolecular ET is very fast compared to k_2 and k_{-2}, the parameters k_R, β, and α given in Table 1 for the EEC(R) model tend to those predicted with the EEC model: $k_R = k_2$, $k_O = k_{-2}$, $\beta = 1$ and $\alpha = 1$. Therefore, when intramolecular *and interfacial* ET are fast, it is simply as if there was no relay.

When Intramolecular ET Is Slow in *Both* Directions, The Signal Consists of Two One-Electron Waves and One of the Catalytic Potentials Is Very Close to the Potential of the Relay. Understanding the case where intramolecular ET is fully rate limiting *in both directions* is more challenging. When k_2 and $k_{-2} \to \infty$, the limiting values of k_R, k_O, β and α are

$$k_R^{lim} = \frac{k_{-1}k'_{-1}}{k_{-1} + k'_{-1}(1+K)} \quad (11a)$$

$$k_O^{lim} = \frac{k_1k'_1}{k_1(1+1/K) + k'_1} \quad (11b)$$

$$\beta^{lim} = X \times \frac{k_{-1}k'_{-1}}{k_1k'_1} \quad (11c)$$

$$\alpha^{lim} = (1+X) \times \frac{k'_{-1}}{k'_1} \quad (11d)$$

$$X = \frac{k_1(1+K) + k'_1K}{k_{-1} + k'_{-1}(1+K)} \geq 0 \quad (11e)$$

Remember that in the case of the EEC(R) model, $K = k_{-2}/k_2$ (cf. Table 1). The term X is positive, but appears to have no obvious physical meaning.

In the Supporting Information, section S3, we show that, in the limit of slow intramolecular ET, the condition given by eq 4 becomes "the wave is a two-electron sigmoid if $X/(1+X)^2 \gg 1$," which cannot be, since X is positive. Therefore, it is not possible to observe a two-electron wave when intramolecular ET is slow in both directions.

Using the relations $k_1/k_{-1} = \exp[f(E_R^0 - E_1^0)]$ and $k'_1/k'_{-1} = \exp[f(E_R^0 - E_2^0)]$, and substituting eqs 11c and 11d into eq 6 with $\alpha' = 0$ gives the following expressions of the catalytic potentials, which are plotted as black lines in Figure 3:

$$E_{cat}^{n=1,red,lim} = E_R^0 - \frac{1}{f}\ln(1+X) \leq E_R^0 \quad (12a)$$

$$E_{cat}^{n=1,ox,lim} = E_R^0 + \frac{1}{f}\ln\left(\frac{1+X}{X}\right) \geq E_R^0 \quad (12b)$$

The difference between E_R^0 and the closest value of $E_{cat}^{n=1,ox,lim}$ or $E_{cat}^{n=1,red,lim}$ is always lower than $(\ln 2)/f$ (the value $(\ln 2)/f$ is reached when $X = 1$, Figure 3). We conclude that when intramolecular ET is slow in both directions, one of the two catalytic potentials is at most 20 mV distant from the potential of the relay. A priori, it would seem that one does not known which of the catalytic potentials is the one that lies close to the potential of the relay, and indeed no information can be obtained from just one CV; however, the dependence of the

dx.doi.org/10.1021/ja311607s | J. Am. Chem. Soc. 2013, 135, 3926−3938

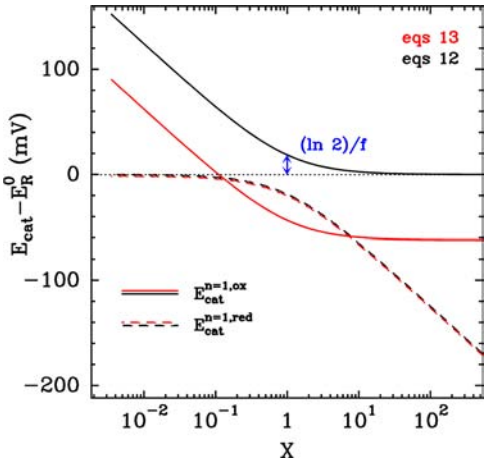

Figure 3. The catalytic potentials plotted against the nondimensional parameter X (defined by eq 11e), when intramolecular ET is slow in both directions (black lines and eqs 12) or when it is slow only in the reductive direction (red lines and eq 13).

catalytic potentials on pH and/or substrate/product/inhibitor concentration may help discriminate.

When Intramolecular ET Is Slow in *Only One* Direction of the Reaction, It Is Unknown if One of the Catalytic Potentials Matches the Potential of the Relay. In Supporting Information section S4, we derive the equations that can be used to understand intermediate situations, or situations where intramolecular ET is rate determining in only one direction of the reaction.

In the general case, we show that two nondimensional parameters, k_O^{lim}/k_{-2} and k_R^{lim}/k_2, determine how the values of E_{cat} vary between the limiting values that are reached when intramolecular ET is either very fast of very slow in both directions. Indeed, the values of β and α are simple functions of these nondimensional parameters (cf. Supporting Information, eqs S12 and S14, respectively).

If, for example, intramolecular ET limits only the reductive reaction ($k_2 \gg k_R^{lim}$ and $k_{-2} \ll k_O^{lim}$), one obtains $\alpha = \alpha^{lim}$ and $\beta = \beta^{lim}k_O^{lim}/k_{-2}$. This leads to the following expressions of the catalytic potentials, which are plotted against X, for $k_{-2}/k_O^{lim} = 0.1$, as red lines in Figure 3:

$$E_{cat}^{n=1,red} = E_R^0 - \frac{1}{f}\ln(1+X) \tag{13a}$$

$$E_{cat}^{n=1,ox} = E_R^0 + \frac{1}{f}\ln\left(\frac{1+X}{X}\right) + \frac{1}{f}\ln(k_{-2}/k_O^{lim}) \tag{13b}$$

The range of values of X for which $E_{cat}^{n=1,red} > E_{cat}^{n=1,ox}$ gives rise to a two-electron wave centered on $E_{cat}^{n=2} = (E_{cat}^{n=1,red} + E_{cat}^{n=1,ox})/2$.

Since there is no reason to assume that X is small or large, we reach the following conclusion: the assumption that intramolecular ET is slow in only one direction of the reaction does not constrain the shape of the wave, nor does it imply that the (or one of the) catalytic potential(s) is close to the reduction potential of the relay.

The One-Electron (EC) Model Is Not a Useful Approximation of the Two-Electron Models. The EC model depicted in Figure 1 is included here for the sake of comparison. The corresponding current equation is plotted in Figure 2a:

$$i = -\frac{F\mathcal{A}\Gamma k_2\left(1 - \frac{k_{-2}}{k_2}e_{one}\right)}{1 + e_{one}} \tag{14}$$

The wave-shape is a "one-electron sigmoid" centered on the one-electron reduction potential of the active site, E_{one}^0; the current goes from $i_{lim}^{red} = -F\,\mathcal{A}\,\Gamma k_2$ at low potential to $i_{lim}^{ox} = +F\,\mathcal{A}\,\Gamma k_{-2}$ at high potential. This model was first treated in ref 15 and used therein to analyze the wave-shapes obtained with hydrogenases, which catalyze the *two-electron* conversion between dihydrogen and protons. The justification was that interfacial ET between the electrode and the enzyme may be fast only up to a certain one-electron redox relay, referred to as the "control center,"[28] which is responsible for the potential-determining step and for giving the wave a one-electron shape. Hereafter, we assess the relevance of this simplification.

We show in Supporting Information section S5 that the shape of a *reversible* two-electron wave (eq 3) becomes indistinguishable from that predicted by the EC model (eq 14) *only* when the following conditions are simultaneously fulfilled:

$$E_{cat}^{n=1,ox} - E_{cat}^{n=1,red} = \frac{\ln 4}{f} \tag{15a}$$

$$K \approx \beta \tag{15b}$$

This is reminiscent of the prediction[4,36−38] that two-electron redox centers give a thin-film voltammetric peak twice that given by a one-electron center if the difference between the two potentials is $(\ln 4)/f$.

We now examine the predictions of the EEC(R) model, to find out whether the two-electron signal takes a "one-electron shape" when intramolecular ET between the relay and the active site is slow in both directions. In that case, eq 12 shows that the two catalytic potentials are separated by $(\ln 4)/f$ on condition that $X = 1$ (X is defined by eq 11e). Therefore, if $\beta \approx K$ (that is, $k_O \approx k_R$) and $X = 1$, then the wave-shape is indeed a *one-electron* sigmoid (Figure 2a,b) centered on the potential of the "control center" (the relay). However, since X is a complex function of many rate constants, it seems unlikely that the very particular situation where $X = 1$ would arise over a large range of experimental conditions (pH, substrate concentration).

More generally, we have shown above that if intramolecular ET is slow in both directions, the signal should consist of two one-electron waves (like in Figure 2e,f), one of which should be close to the potential of the relay, whereas any shape and position of the wave can be observed if intramolecular ET is slow in only one direction of the reaction.

Therefore, the concept of "control center"[11,15,28] does not appear to be useful when the enzyme can catalyze the reaction in both directions.

The Greater Is the Current in One Direction, The Greater Is the Corresponding Overpotential. The overpotential (η) for either the oxidative or the reductive reaction is a phenomenological parameter that evaluates the energetic efficiency of the catalyst. It is loosely defined as the absolute value of the difference between the OCP and the potential at which a current is experimentally observed; we define the latter as the catalytic potential. This definition is the same as that in ref 39 since the catalytic potential is the half-wave potential. Alternatively, one may define the overpotential by "how much driving force is required to get a certain current density". The latter definition is appropriate to electrode materials, but not to

dx.doi.org/10.1021/ja311607s | J. Am. Chem. Soc. 2013, 135, 3926−3938

molecular catalysts (see discussion in reference 39). The definition we use, based on the "mid-point potential", reports on features of the voltammetric response, not on its magnitude.

Equation 3 can be used to discuss the contribution to the overpotential of the chemical reactions, and the relations between the values of the limiting currents and overpotentials in the two directions of the reaction.

Although the equations herein have been derived for adsorbed catalysts, they can also be used for discussing the data obtained with a freely diffusing catalyst. Indeed, the overpotential of the latter includes contributions arising from mass transport and can only be greater than that of the adsorbed catalyst.

We examine two cases depending on whether the signal consists of a single 2-electron wave or two one-electron waves (Figure 2). The case of a single 2-electron wave is simple: if the reductive and the oxidative limiting currents are of the same magnitude, then there is essentially no overpotential in either direction (cf. Figure 2c,d); if, on the other hand, this wave displays significant current in only one direction (this case is not illustrated in Figure 2), the overpotential for that reaction is given by

$$\eta = \left| E_{\mathrm{cat}}^{n=2} - E_{\mathrm{OCP}} \right| = \frac{1}{2f} \left| \ln \frac{k_O}{k_R} \right| \tag{16}$$

(eq 16 is obtained from eqs 5 and 10a). In other words, for a 2-electrons wave, the greater the catalytic bias, the greater the overpotential; this is a direct consequence of the fact that the 2-electron waveshape is very simple.

When the signal consists of two distinct one-electron waves (as in Figure 2e,f), combining eqs 6 and 10a gives

$$\eta^{\mathrm{ox}} = E_{\mathrm{cat}}^{n=1,\mathrm{ox}} - E_{\mathrm{OCP}} = \eta_i + \frac{1}{2f} \ln \frac{k_{\mathrm{O}}}{k_{\mathrm{R}}} \tag{17a}$$

$$\eta^{\mathrm{red}} = E_{\mathrm{OCP}} - E_{\mathrm{cat}}^{n=1,\mathrm{red}} = \eta_i - \frac{1}{2f} \ln \frac{k_{\mathrm{O}}}{k_{\mathrm{R}}} \tag{17b}$$

(η_i is defined below in eq 18). The overpotential is composed of two terms. Just like in the 2-electron case, it includes a term which depends on the bias and penalizes the direction where the catalysis is the fastest. It also includes a term that applies to both directions,

$$\eta_i = \frac{1}{f} \ln \frac{(\alpha\delta + \alpha'/\delta)}{\sqrt{\beta}} \tag{18}$$

According to eq 4, η_i is always positive when the signal consists of two 1-electron waves. This term has a simple thermodynamic meaning in the case of the EEC model (where, according to Table 1, $\alpha' = 0$, $\alpha = \beta = 1$):

$$\eta_i^{\mathrm{EEC}} = \frac{1}{f} \ln \delta = \frac{E_1^0 - E_2^0}{2} \tag{19}$$

It can be interpreted thus: a stable half-reduced intermediate is a thermodynamic sink that makes the overpotential large in both directions.[21] For more complex models however, the overpotential is not a thermodynamic quantity; instead, it depends on the values of rate constants. For the EECC model for instance, η_i reads

$$\eta_i^{\mathrm{EECC}} = \frac{E_1^0 - E_2^0}{2} - \frac{1}{2f} \ln \left[\left(1 + \frac{k_1}{k_2 + k_{-1}} \right) \left(1 + \frac{k_{-2}}{k_2 + k_{-1}} \right) \right] \tag{20}$$

Equation 20 shows that accumulating the intermediate that is produced between the two chemical steps (X_2 in Figure 1) by increasing the rate of its formation (k_1 and/or k_{-2}) decreases the overpotential; this makes sense as increasing k_1 (respectively, k_{-2}) pulls the A_I/A_R (respectively, A_O/A_I) equilibrium in favor of A_R (respectively, A_O), which destabilizes the half-reduced active site. This effect may compensate for the difference $E_1^0 - E_2^0$ being large.

A general consequence is drawn from eqs 17: when the signal consists of two 1-electron waves, the wave with the larger current is always the one with the greater overpotential.

Unlike inorganic chemists, electrochemists sometimes define the overpotential as $\eta = E - E_{\mathrm{OCP}}$, that is, the ordinate in a Tafel plot. Based on that definition, an analysis is presented in ref 40 to evaluate the efficiency of an irreversible catalyst by extrapolating the turnover frequency to $\eta = 0$. This method could be applied to an adsorbed redox enzyme, on condition that Γ and i_{lim} are known.

Slow Interfacial Electron Transfer Broadens the Signals Predicted by the EC, EEC, ECEC and EECC Models. When interfacial ET is not very fast on the time scale of turnover, the redox centers in the enzyme are not in Nernstian equilibrium with the electrode. Slow interfacial ET broadens the catalytic wave, as described below, but the positions of the main features of the wave should be no different from those calculated in the Nernstian limit (unless interfacial ET is so slow compared to catalytic turnover that the signal loses all distinctive features).

We describe interfacial ET kinetics using the Butler–Volmer model, assuming that all transfer coefficients equate to $^1/_2$; we note k_1^0 and k_2^0, the rates of ET at zero overpotential, that correspond to the redox couples numbered 1 and 2 in Figure 1, and $\kappa = k_2^0/k_1^0$. When interfacial ET is taken into account, eq 2 has an additional term in the denominator:

$$i = -\frac{nF\mathcal{A}\Gamma k_{\mathrm{R}}(1 - a')}{a + k_{\mathrm{R}}/k_1^0 b} \tag{21}$$

where b is a nondimensional function defined for each model in Supporting Information, Table S1; the term b includes half-integer powers of e_1 and e_2 and depends on κ. Of course the Nernstian limit (eq 2) is recovered when k_{R}/k_1^0 is small.

To obtain a current equation that can describe real situations, the dispersion of interfacial ET transfer that results from the fact that not all enzymes are immobilized in exactly the same orientation must be taken into account.[30] Based on simple geometrical considerations (section 2.2.5.4 in ref 4), the distribution of orientations is predicted to be such that, within a certain range, all of the possible distances d between the electrode surface and the exposed relay where the electrons come in and out of the enzyme occur with the same probability. The difference between the largest and the smallest distance is d_0. The distribution of k^0 values is obtained by taking into account the exponential dependence of k^0 on distance, $k^0(d) = k^{0,\max} \exp(-\beta^{\mathrm{ET}} d)$ where $k^{0,\max}$ is the rate of interfacial ET that corresponds to the shortest distance. Equation 21 is easily integrated across all possible values of k^0, using the property

that b is the same for all adsorbed molecules, even if their orientations differ:[30]

$$i = -\frac{nF\mathcal{A}\Gamma k_R(1-a')}{a}\left[1 + \frac{1}{\beta^{ET}d_0}\ln\frac{a + \frac{k_R}{k^0}b}{a + \frac{k_R}{k^0}b\exp(\beta^{ET}d_0)}\right] \quad (22)$$

Equation 22 was used to calculate the signals shown on the right column of Figure 2. It predicts that there are ranges of potential where the current−potential relation is linear (dashed red segments in Figure 2b,d,f). This linear change in catalytic current at high driving force results from the response of enzyme molecules having low k^0 values with respect to the turnover rate, which contribute only at high driving force.[30]

In experiments, it is often observed that the current keeps increasing linearly at high driving force without reaching the oxidative and reductive limits. This corresponds to the following approximation of eq 22, obtained in the limit $\beta^{ET}d_0 \to \infty$:

$$i = -nF\mathcal{A}\Gamma\frac{k_R}{\beta^{ET}d_0}\frac{1-a'}{a}\ln\left[1 + \frac{k^0 a}{k_R b}\right] \quad (23)$$

Note that in eq 23, k_R and $\beta^{ET}d_0$ appear only as a ratio and can therefore not be determined independently. The slopes of the linear parts of the voltammograms are:

$$\frac{di}{dE} \propto \frac{nF^2\mathcal{A}\Gamma k_R}{2RT\beta^{ET}d_0} \text{ at low potential} \quad (24a)$$

$$\frac{di}{dE} \propto \frac{nF^2\mathcal{A}\Gamma k_O}{2RT\beta^{ET}d_0} \text{ at high potential} \quad (24b)$$

We conclude that the limiting *slopes* are proportional to the limiting *currents* that are not reached and can therefore not be measured; however, the catalytic bias (k_R/k_O) can be simply measured from the ratio of limiting slopes.

The EEC, ECEC, and EECC models are indiscernible, and the meaning of the catalytic potentials is model-dependent. Importantly, the wave-shape alone cannot be used to discriminate between the three models. Indeed, in the Nernstian limit, the corresponding current equations (eq 3) all take the exact same form:

$$i = -\frac{2F\mathcal{A}\Gamma k_R\left(1 - \frac{K}{\beta}e_0'^2\right)}{1 + K_{disp}^{-1/2}e_0' + e_0'^2} \quad (25)$$

where $e_0' = \exp[f(E - E_{cat}^{n=2})]$ and K_{disp} is defined by eq 4. Therefore, in the Nernstian limit, the current equation depends on a prefactor which defines the magnitude of the wave, and on three independent parameters that entirely define its shape. An example of set of parameters is the average catalytic potential $E_{cat}^{n=2}$, the apparent disproportionation constant and the bias $k_O/k_R = K/\beta$. Another set of independent parameters could be $E_{cat}^{n=1,red}$, $E_{cat}^{n=1,ox}$ and the bias (we chose this when we analyzed the data in Figures 5 and 6).

The term b, which accounts for slow interfacial ET in eqs 21−23, does not resolve the ambiguity between the different models. Indeed, for all three models, Supporting Information, Table S1 shows that it has the same form and dependence on potential, with two additional parameters that are complex combinations of rate constants:

$$\frac{k_R}{k_1^0} \times b \equiv \frac{k_R^{app}}{k_1^0}e_0'^{1/2} + \frac{k_O^{app}}{k_1^0}e_0'^{3/2} \quad (26)$$

The fact that all three models give the same rate equation (not only in the Nernstian limit) has the following fundamental consequence: the EEC model gives an equation that is both simple and useful, provided it is acknowledged that it only returns the values of "catalytic potentials," the meaning of which is entirely model dependent. There is no reason to assume that these catalytic potentials directly report on the reduction potentials of the active site. For example, eq 5 shows that $E_{cat}^{n=2}$ departs from E_0^0 unless $\beta = 1$. Obviously, this is a serious limitation to the interpretation of the catalytic waves.

The ambiguity of the physical meaning of the parameters in the rate equation is a very common situation in enzyme kinetics: for example, it well-known that many distinct enzymatic mechanisms can give the Michaelis−Menten rate equation, and that the meaning of the Michaelis constants (v_{max} and K_m) depends on which model is considered: a value of K_m may depart from the corresponding dissociation constant, but whether or not it does cannot be established based on steady-state kinetics alone.[41]

On a more positive note, we believe that a case-by-case quantitative interpretation of the dependence of the catalytic potentials and limiting currents on pH and substrate concentration should make it possible to discriminate between the different models and to give a physical meaning to these empirical parameters. This work is in progress in our lab with the different enzymes with which we work , but it is out of the scope of this paper.

The EEC(R) and EEC Models Give Distinct Rate Equations if Interfacial ET Is Not Too Fast. Taking simultaneously into account the effects of interfacial and intramolecular ET is laborious but rewarding. The rate equation for the EEC(R) model cannot be given the form of eq 21 (see Supporting Information section S6). The expression can nonetheless be integrated across all possible values of k_0 to give an expression that takes into account the distribution of orientations, and can be used to analyze the data:

$$i = \frac{\alpha_1}{\alpha_2}\left[\ln\frac{\Gamma_1}{\Gamma'_1} + \frac{\alpha_3}{\alpha_4} \times \tanh^{-1}\frac{\alpha_4(\Gamma_2 - \Gamma'_2)}{\alpha_4^2 - \Gamma_2\Gamma'_2}\right] \quad (27)$$

where both α_i and Γ_i depend on potential and on the rate constants in the model, but only the parameters Γ_i depend on k^0; the unprimed versions of the parameters Γ_i are taken at the maximum value of k^0, $k^{0,max}$, while the primed values of Γ_i are taken at the minimum value $k^{0,max}\exp(-\beta^{ET}d_0)$. In Supporting Information section S6, we give the relations between the parameters in eq 27 and the rate constants of the EEC(R) kinetic scheme. In Supporting Information S7, we give the condition for the equivalence between the EEC and EEC(R) models.

Importantly, eq 27 is distinct from eq 22, which suggests that it is possible to deduce from the shape of the voltammogram whether electron transfer is mediated by an internal relay.[42] We do so hereafter, by comparing the steady-state catalytic signatures of the FeFe hydrogenases from *C. reinhardtii* and *C. acetobutylicum*.

dx.doi.org/10.1021/ja311607s | J. Am. Chem. Soc. 2013, 135, 3926−3938

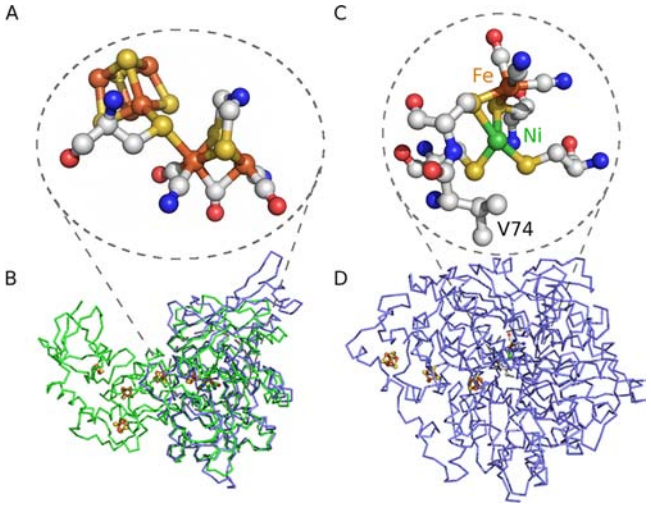

Figure 4. The X-ray structures of the hydrogenases studied here. Panel A shows the FeFe active site "H-cluster" which is the same in the two hydrogenases whose backbones are overlaid in panel B. Panel B shows the backbones of the enzymes from *Clostridium acetobutylicum* (green trace, modeled from the structure of *C. pasteurianum* hydrogenase, pdb 3C8Y, ref 23) and *Chlamydomonas reinhardtii* (blue trace, pdb 3LX4, ref 24). Panels C and D show the active site and the backbone of the NiFe hydrogenase from *D. fructosovorans*. The Valine 74 that blocks the substrate gas channel[43] is also indicated (pdb 1YQ9 for the WT enzyme, and 3H3X for the V74 M mutant[44] studied here). The chains of FeS clusters that are used for long-range electron transfer are visible in panels B and D.

The Electrochemical Signals Obtained with Two Structurally Distinct FeFe Hydrogenases Reveal the Presence or Absence of a Relay. Figure 4B shows the structure of two different hydrogenases which share the same active site, the "H-cluster" which is shown in Panel A. The H-cluster consists of a $[Fe_2(CO)_3(CN)_2(dtma)]$ subsite[45] (dtma=dithiomethylamine) covalently bound to a [4Fe4S] subcluster. Which three states of the active site are part of the catalytic cycle has been debated. There is an agreement about the fact that the so-called Hox and Hred states ($Fe^{II}Fe^{I}$-$[4Fe4S]^{2+}$ and $Fe^{I}Fe^{I}$-$[4Fe4S]^{2+}$, respectively) are involved in catalysis; the third catalytic intermediate is either more oxidized than Hox[46] or more reduced than Hred.[47] In any case, the [4Fe4S] subcluster is part of the active site, instead of playing the role of an electron relay used for electron entry, exit, and storage.

The enzyme from the green algae *Chlamydomonas reinhardtii* is the smallest hydrogenase purified so far. Its backbone is shown in blue in Figure 4B. It has a molecular weight of 49 kDa and no cofactor other than the H-cluster, which is exposed at the surface of the protein. In contrast, the enzyme from *Clostridium acetobutylicum* has a 200-amino acid N-terminal extension, which covalently binds four additional FeS clusters (total M_w 64 kDa, green in Figure 4B), two of which are exposed at the protein surface. They mediate long-range electron transfer, as occurs in many other redox enzymes.[10,35] Both FeFe hydrogenases have a surface patch of basic residues that can be used for covalent attachment and direct ET to graphite electrodes modified with a carboxybenzene moiety.[48]

Figure 5 shows the cyclic voltammograms (panels A and B) and the first derivatives of the data (panels C and D) obtained with the enzymes from *Chlamydomonas reinhardtii* (left column) and *Clostridium acetobutylicum* (right column), in a solution at 30 °C, pH 7, saturated with H_2. The electrode rotation rate was high to avoid mass transport control (this would artificially flatten the voltammogram). To ensure steady-state, the scan rate was low (20 mV/s) and the potential was kept below 0 V vs SHE (the enzyme slowly and reversibly inactivates under very oxidative conditions.[15,47]) The contribution of the capacitive current was so small in these experiments (± 0.2 μA) that it could be removed simply by averaging the forward and backward currents.

The red and blue lines in figure 5 show the fits of the EEC and EEC(R) models to the data (eqs 23 and 27, respectively). Fitting the models required simultaneously adjusting five or eight parameters, whose "best" values are listed in Supporting Information section S8. We found that reliable parameters could only be obtained provided the model was simultaneously fit to the data and their first derivative, as illustrated in Figure 5. In contrast, attempts to fit the model to only the voltammogram were often unsuccessful: for example we observed that the results were dependent on the initial guess in the fitting procedure, or the fitting algorithm[49] returned large errors on the values of the adjusted parameters *and* the covariance matrices showed that they were correlated. None of these problems arose when we simultaneously modeled the data and their derivative.

Regarding the enzyme from *Chlamydomonas reinhardtii*, which houses only the active site H-cluster (left column in Figure 5), the EEC model (red) is better than the EEC(R) model (blue) *despite the fact* that the latter model has three more adjustable parameters than the former. In the case of the enzyme from *Clostridium acetobutylicum*, which has a chain of redox relays, the opposite situation is observed, with the EEC(R) model (blue) being better than the EEC model (red) (right column in Figure 5), as expected from the structure and cofactor content of each enzyme (Figure 4).

Although the differences between the two fits are small, two observations strengthened our conclusions. First, we found that the EEC and EEC(R) models better describe the data obtained with the enzymes from *C. reinhardtii* and *C. acetobutylicum*, respectively, irrespective of the pH in the range 5 to 8. The second observation concerns the analysis of the *C. acetobutylicum* data: when the pH is varied, the OCP and the overall position of the wave shifts −60 mV per pH unit, but the value of the reduction potential of the relay, which is one of the parameters of the fit, shows much weaker pH dependence (about −20 mV per pH unit); a weak dependence on pH is what one expects for the reduction potential of an electron transferring FeS cluster. The value we obtained was $E^0_R \approx -450$ mV vs SHE at pH 7, but unfortunately, it cannot be compared to the result of a redox titration: the thermodynamics of the ET chain in *C. acetobutylicum* hydrogenase is not known yet.

The Data Obtained with Two NiFe Hydrogenases Illustrate the Relation between Bias and Catalytic Potential. The structure of the WT form of the NiFe hydrogenase from *D. fructosovorans*, is shown in Figure 4C,D. The active site is a dinuclear cluster of Ni and Fe which is attached to the protein by four cysteine residues. It is usually considered that the catalytic cycle involves three different spectroscopically characterized redox states of the active site called NiSI, NiC, and NiR.[50] Valine 74 (panel C) is located near the active site, at the end of a network of hydrophobic cavities that guide the diffusion of H_2 toward and from the solvent.[43,51] Replacing V74 with a methionine has no effect on the structure and chemistry of the active site,[44] but it slows

dx.doi.org/10.1021/ja311607s | J. Am. Chem. Soc. 2013, 135, 3926−3938

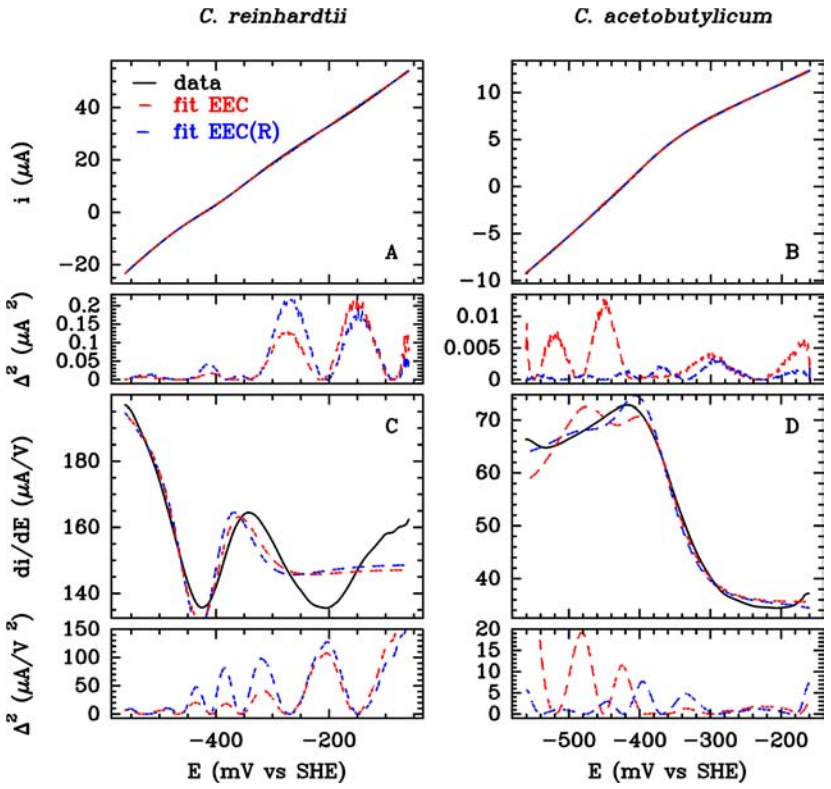

Figure 5. Catalytic signals (H_2 oxidation at high potential, and production at low potential) for *C. reinhardtii* and *C. acetobutylicum* FeFe hydrogenases covalently attached to a rotating disc graphite electrode (plain black line). T = 30 °C, pH 7, 1 bar H_2, ω = 3 krpm, 20 mV/s. Panels A and B show the steady-state voltammograms (after correction for the capacitive current) and panels C and D the first derivative of the data. The dashed red and blue lines are the best fits using the EEC and EEC(R) models, respectively. The small panels show the squared residues for each fit. The values of the optimized parameters and corresponding errors are listed in Supporting Information section S8.

down intramolecular diffusion of all ligands (O_2, CO, and H_2) by orders of magnitude.[5] As a consequence, the enzyme becomes a much more efficient catalyst of H_2 oxidation than production.[14]

Figure 6 shows data obtained with the WT (left column) and V74M variant (right column) of *D. fructosovorans* NiFe hydrogenase. The V74M voltammogram clearly shows that the mutant is biased to operate in the oxidative direction (simply compare the magnitudes of the positive and negative currents). According to eq 10a, a modification that affects the enzyme's catalytic bias should also change the position of the catalytic wave (the "catalytic potential"), and indeed, the V74M mutation shifts the wave toward high potential. However, this cannot be taken as evidence that the mutation has modified the reduction potential of the active site (see above).

We analyzed the NiFe hydrogenase data with the EEC and EEC(R) models, but unlike the case of FeFe hydrogenases (Figure 5) we could not obtain any evidence that the fits to the EEC(R) model were better than that to the simpler EEC model. The reason becomes obvious when one examines the fits to the EEC model shown in Figure 6: the residue is already very small, of the order of 5 nA, which is actually much smaller than the capacitive current (about ±200 nA). The fits to the EEC(R) data (not shown) were just as good, and the very small difference between the two residuals is meaningless.

It is remarkable that in all cases (including FeFe hydrogenases), the values of E_1^0 and E_2^0 obtained with the EEC model matched (within a few millivolts) the values calculated using the EEC(R) model and the relations $E_1^0 = E_R^0 + 1/f\ln(k_{-1}/k_1)$ and $E_2^0 = E_R^0 + 1/f\ln(k'_{-1}/k'_1)$ (Figures 5, 6 and Supporting Information sections S8 and S9). This agreement between the values obtained with the two models shows that the positions of the main features of the catalytic waves determine the values of the catalytic potentials, which can be evaluated when the data are less accurate with the EEC even when the enzyme has an electron transfer chain (in which case, the EEC(R) model would be more appropriate).

Last, we note that the results of the analysis of all data with the EEC(R) model indicate that intramolecular ET is fast (the parameters k_1/k_2 and k'_1/k_2 measure the ratio of rate of intramolecular ET over rate of active site chemistry; their values are very large and ill-defined).

■ CONCLUSIONS AND PERSPECTIVES

Over the past few years, protein film voltammetry has proved very useful for studying the inhibition, and (in)activation of various enzymes under *potentiostatic* conditions because chronoamperometric data are usually very easy to interpret in a quantitative manner.[5,8,52−54] Understanding the dependence of activity on potential is another matter altogether. Yet, voltammetric data embed the information relevant to understanding the catalytic mechanism, and one should make the effort to develop rigorous models of steady-state wave shapes that can be used to learn about catalysis by redox enzymes and electrocatalysts.

In this paper, we have thoroughly discussed the interpretation of the wave-shapes obtained with two-electron, reversible electrocatalysts. We found that the one-electron rate equation is not a useful approximation, even when intramolecular electron transfer is slow. When intramolecular ET limits turnover in

dx.doi.org/10.1021/ja311607s | J. Am. Chem. Soc. 2013, 135, 3926−3938

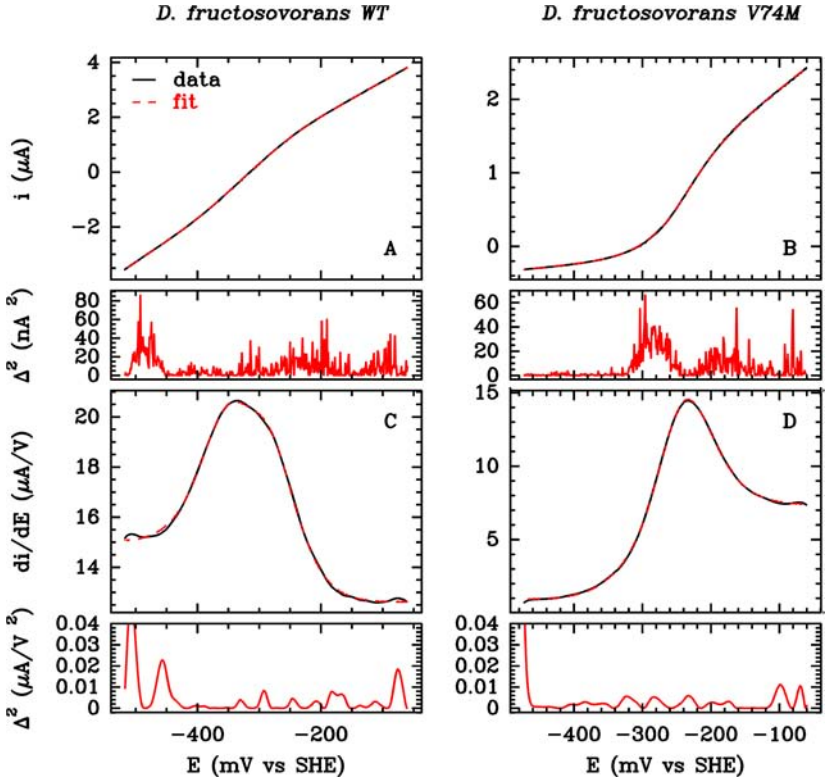

Figure 6. Catalytic signals (H_2 oxidation at high potential, and production at low potential) for *D. fructosovorans* WT and *D. fructosovorans* V74 M NiFe hydrogenases covalently attached to a rotating disc graphite electrode (plain black line). T = 40 °C, pH 5.5, 0.1 bar H_2, ω = 3 krpm, 10 mV/s. The data are the same as in ref 14. Panels A and B show the steady-state voltammograms (after correction for the capacitive current) and panels C and D the first derivative of the data. The dashed red lines are the best fits using the EEC model. The small panels show the residues for each fit. The values of the optimized parameters are listed in Supporting Information, together with the values of the parameters obtained by analyzing the data with the EEC(R) model.

both directions of the reaction (that is, when this relay is the "control center"), the signal should consist of two one-electron waves, one of which is close to the potential of the control center. No such simple prediction can be made if intramolecular ET limits turnover in only one direction of the reaction. Only in very specific situations will the catalytic potentials, deduced from the analysis of the data with an EEC model, equate to the reduction potentials of the active site; one consequence of this is that there is no simple relation between the thermodynamic properties of the active site and the catalytic bias of the enzyme.[14] When interfacial ET is not very fast (that should be in most cases), the wave-shape may reveal the presence of an electron transfer relay, even if intramolecular ET is not rate-limiting.

We are now studying further the voltammograms obtained with various hydrogenases, and examining the dependence on pH and H_2 pressure of the parameters of the fits, to learn about the sequences of events (substrate binding and release, proton and electron transfers) that occur in the catalytic cycle of these enzymes.

METHODS

Samples of *C. acetobutylicum* and *C. reinhardtii* FeFe hydrogenases were prepared as described in refs 54−56. Reference 48 fully describes the procedure for attaching these enzymes to rotating disc pyrolytic graphite edge electrodes (RDPGE). The purification of the enzymes from *D. fructosovorans* and the procedure for covalent attachment are described in refs 5, 8, and 57.

Protein film electrochemistry experiments were carried out in a glovebox filled with N_2, using the electrochemical setup and equipment previously described.[5] The two-compartment electrochemical cell was kept at the desired temperature value using a water circulation system. The RDPGE (area $\mathcal{A} \approx 3$ mm^2) was used in conjunction with an electrode rotator, a platinum wire was used as a counter electrode, and a saturated calomel electrode (SCE), located in a side arm containing 0.1 M NaCl and maintained at room temperature, was used as a reference. All potentials are quoted versus the standard hydrogen electrode (SHE), ($E_{SHE} = E_{SCE} + 240$ mV). The electrochemical cell contained a buffer mixture of MES, CHES, TAPS, HEPES, and sodium acetate (5 mM each), 1 mM EDTA, and 0.1 M NaCl.

We analyzed and fit the data using in-house programs called SOAS,[58] and QSoas. The former is available free and free of charge on our Web site at http://bip.cnrs-mrs.fr/bip06/software.html. It is being replaced by an entirely new, powerful, open program called QSoas, which will become available soon. Both programs embed the ODRPACK software for distance regression,[49] but QSoas has much more flexible fitting procedures, which make it possible, for example, to simultaneously model a data set and its derivative; this proved crucial in this study. Check our web pages for updates or follow us on twitter (https://twitter.com/BIP6_Marseille).

ASSOCIATED CONTENT

Supporting Information

Supplementary Table S1. Section S1: complete lists of authors for refs 5, 43, 44, 54. Section S2: derivation of eqs 5 and 6. Section S3: condition for obtaining a two electron wave when intramolecular ET is slow in both directions. Section S4: EEC(R) model when ET is slow in only one direction. Section S5: demonstration of eq 15, that is, conditions for the equivalence between the EC and EEC models. Section S6:

demonstration of eq 27, the EEC(R) rate equation when the wave is broaden by slow interfacial ET. Section S7: condition for the equivalence between the EEC(R) and EEC models. Sections S8 and S9: parameters obtained from the fits in Figures 5 and 6. Section S10: list of symbols, in order of appearance in main text. This material is available free of charge via the Internet at http://pubs.acs.org.

AUTHOR INFORMATION

Corresponding Author

christophe.leger@imm.cnrs.fr

Notes

The authors declare no competing financial interest.

ACKNOWLEDGMENTS

Our work is funded by the CNRS, CEA, Aix-Marseille Univ, ANR (ANR-12-BS08-0014- 01), City of Marseilles and, Région Provence Alpes Cote d'Azur (PACA). We acknowledge support from the "Pôle de compétitivite Capénergie". A.A.H. thanks the CNRS and Region PACA for funding his PhD.

REFERENCES

(1) Berezin, I. V.; Bogdanovskaya, V. A.; Varfolomeev, S. D.; Tarasevich, M. R.; Yaropolov, A. I. *Dokl. Akad. Nauk. USSR* **1978**, *240*, 615−618.

(2) Tarasevich, M. R.; Yaropolov, A. I.; Bogdanovskaya, V. A.; Varfolomeev, S. D. *J. Electroanal. Chem. Interfacial Electrochem.* **1979**, *104*, 393−403.

(3) Yaropolov, A. I.; Karyakin, A. A.; Varfolomeev, S. D.; Berezin, I. V. *Bioelectrochem. Bioenerg.* **1984**, *12*, 267−277.

(4) Léger, C.; Bertrand, P. *Chem. Rev.* **2008**, *108*, 2379−2438.

(5) Liebgott, P.-P.; et al. *Nat. Chem. Biol.* **2010**, *6*, 63−70.

(6) Fourmond, V.; Sabaty, M.; Arnoux, P.; Bertrand, P.; Pignol, D.; Léger, C. *J. Phys. Chem. B* **2010**, *114*, 3341−3347.

(7) Abou-Hamdan, A.; Liebgott, P.-P.; Fourmond, V.; Gutierrez-Sanz, O.; Lacey, A. L. D.; Infossi, P.; Rousset, M.; Dementin, S.; Leger, C. *Proc. Natl. Acad. Sci. U.S.A.* **2012**, *109*, 19916−19921.

(8) Abou Hamdan, A.; Burlat, B.; Gutierrez-Sanz, O.; Liebgott, P.; Baffert, C.; de Lacey, A.; Rousset, M.; Guigliarelli, B.; Leger, C.; Dementin, S. *Nat. Chem. Biol.* **2013**, *9*, 15−17.

(9) Léger, C.; Heffron, K.; Pershad, H. R.; Maklashina, E.; Luna-Chavez, C.; Cecchini, G.; Ackrell, B. A. C.; Armstrong, F. A. *Biochemistry* **2001**, *40*, 11234−11245.

(10) Page, C. C.; Moser, C. C.; Chen, X.; Dutton, P. L. *Nature* **1999**, *402*, 47−52.

(11) Léger, C.; Lederer, F.; Guigliarelli, B.; Bertrand, P. *J. Am. Chem. Soc.* **2006**, *128*, 180−187.

(12) Butt, J. N.; Filipiak, M.; Hagen, W. R. *Eur. J. Biochem.* **1997**, *245*, 116−122.

(13) Pershad, H. R.; Hirst, J.; Cochran, B.; Ackrell, B. A. C.; Armstrong, F. A. *Biochim. Biophys. Acta* **1999**, *1412*, 262−272.

(14) Abou Hamdan, A.; Dementin, S.; Liebgott, P.-P.; Gutierrez-Sanz, O.; Richaud, P.; De Lacey, A. L.; Roussett, M.; Bertrand, P.; Cournac, L.; Léger, C. *J. Am. Chem. Soc.* **2012**, *134*, 8368−8371.

(15) Hexter, S. V.; Grey, F.; Happe, T.; Climent, V.; Armstrong, F. A. *Proc. Natl. Acad. Scl. U.S.A.* **2012**, *109*, 11516−11521.

(16) Dementin, S.; Belle, V.; Bertrand, P.; Guigliarelli, B.; Adryanczyk-Perrier, G.; Delacey, A.; Fernandez, V. M.; Rousset, M.; Léger, C. *J. Am. Chem. Soc.* **2006**, *128*, 5209−5218.

(17) Yang, J. Y.; Chen, S.; Dougherty, W. G.; Kassel, W. S.; Bullock, R. M.; DuBois, D. L.; Raugei, S.; Rousseau, R.; Dupuis, M.; DuBois, M. R. *Chem. Commun.* **2010**, *46*, 8618−8620.

(18) Tran, P. D.; Le Goff, A.; Heidkamp, J.; Jousselme, B.; Guillet, N.; Palacin, S.; Dau, H.; Fontecave, M.; Artero, V. *Angew. Chem., Int. Ed.* **2011**, *50*, 1371−1374.

(19) Heering, H. A.; Hirst, J.; Armstrong, F. A. *J. Phys. Chem. B* **1998**, *102*, 6889−6902.

(20) Bertrand, P.; Frangioni, B.; Dementin, S.; Sabaty, M.; Arnoux, P.; Guigliarelli, B.; Pignol, D.; Léger, C. *J. Phys. Chem. B* **2007**, *111*, 10300−10311.

(21) Koper, M. T.; Bouwman, E. *Angew. Chem., Int. Ed.* **2010**, *49*, 3723−3725.

(22) De Lacey, A. L.; Fernández, V. M.; Rousset, M.; Cammack, R. *Chem. Rev.* **2007**, *107*, 4304−4330.

(23) Pandey, A. S.; Harris, T. V.; Giles, L. J.; Peters, J. W.; Szilagyi, R. K. *J. Am. Chem. Soc.* **2008**, *130*, 4533−4540.

(24) Mulder, D. W.; Boyd, E. S.; Sarma, R.; Lange, R. K.; Endrizzi, J. A.; Broderick, J. B.; Peters, J. W. *Nature* **2010**, *465*, 248−251.

(25) Léger, C.; Jones, A. K.; Roseboom, W.; Albracht, S. P. J.; Armstrong, F. A. *Biochemistry* **2002**, *41*, 15736−15746.

(26) Heering, H. A.; Hirst, J.; Armstrong, F. A. *J. Phys. Chem. B* **1998**, *102*, 6889−6902.

(27) Reda, T.; Hirst, J. *J. Phys. Chem. B* **2006**, *10*, 1394−1404.

(28) Elliott, S. J.; McElhaney, A. E.; Feng, C.; Enemark, J. H.; Armstrong, F. A. *J. Am. Chem. Soc.* **2002**, *124*, 11612−11613.

(29) Bard, A. J.; Faulkner, L. R. *Electrochemical Methods. Fundamental and Applications*, 3rd ed.; John Wiley & Sons, Inc.: New York, 2004.

(30) Léger, C.; Jones, A. K.; Albracht, S. P. J.; Armstrong, F. A. *J. Phys. Chem. B* **2002**, *106*, 13058−13063.

(31) The effect of fast coupled reactions on E^0 and k^0 has been thoroughly discussed in a series of papers written by Etienne Laviron in the 1980s,[32,33] see also ref 34 and section 2.1.2.1 in ref 4.

(32) Laviron, E. *J. Electroanal. Chem.* **1980**, *109*, 57−67.

(33) Meunier-Prest, R.; Laviron, E. *J. Electroanal. Chem.* **1992**, *328*, 33−46.

(34) Anxolabéhère-Mallart, E.; Costentin, C.; Policar, C.; Robert, M.; Savéant, J.-M. M.; Teillout, A.-L. L. *Faraday Discuss.* **2011**, *148*, 83−95.

(35) Dementin, S.; Burlat, B.; Fourmond, V.; Leroux, F.; Liebgott, P.-P. P.; Abou Hamdan, A.; Léger, C.; Rousset, M.; Guigliarelli, B.; Bertrand, P. *J. Am. Chem. Soc.* **2011**, *133*, 10211−10221.

(36) Michaelis, L.; Schubert, M. P. *Chem. Rev.* **1938**, *22*, 437−470.

(37) Plichon, V.; Laviron, E. *J. Electroanal. Chem.* **1976**, *71*, 143−156.

(38) Savéant, J. M. *Elements of Molecular and Biomolecular Electrochemistry*; John Willey & Sons, Inc.: New York, 2006.

(39) Fourmond, V.; Jacques, P.-A.; Fontecave, M.; Artero, V. *Inorg. Chem.* **2010**, *49*, 10338−10347.

(40) Costentin, C.; Drouet, S.; Robert, M.; Savéant, J. M. *J. Am. Chem. Soc.* **2012**, *134*, 11235−11242.

(41) Cornish-Bowden, A. *Fundamentals of Enzyme Kinetics*; Portland Press.: London, 2004.

(42) Note that in contrast, in the Nernstian limit, all five two-electron models give the same rate equation.

(43) Leroux, F.; et al. *Proc. Nat. Acad. Sc. U.S.A.* **2008**, *105*, 11188−11193.

(44) Dementin, S.; et al. *J. Am. Chem. Soc.* **2009**, *131*, 10156−10164.

(45) Silakov, A.; Wenk, B.; Reijerse, E.; Lubitz, W. *Phys. Chem. Chem. Phys.* **2009**, *11*, 6592−6599.

(46) Greco, C.; Bruschi, M.; De Gioia, L.; Ryde, U. *Inorg. Chem.* **2007**, *46*, 5911−5921.

(47) Adamska, A.; Silakov, A.; Lambertz, C.; Rüdiger, O.; Happe, T.; Reijerse, E.; Lubitz, W. *Angew. Chem., Int. Ed.* **2012**, *51*, 11458−11462.

(48) Baffert, C.; Sybirna, K.; Ezanno, P.; Lautier, T.; Hajj, V.; Meynial-Salles, I.; Soucaille, P.; Bottin, H.; Léger, C. *Anal. Chem.* **2012**, *84*, 7999−8005.

(49) Boggs, P. T.; Donaldson, J. R.; Richaard; Schnabel, R. B. *Assoc. Comput. Machin. Trans. Math. Software* **1989**, *15*, 348−364.

(50) Pandelia, M.-E.; Fourmond, V.; Tron-Infossi, P.; Lojou, E.; Bertrand, P.; Léger, C.; Giudici-Orticoni, M.-T.; Lubitz, W. *J. Am. Chem. Soc.* **2010**, *132*, 6991−7004.

(51) Wang, P.-H.; Blumberger, J. *Proc. Nat. Acad. Sc. U.S.A.* **2012**, *109*, 6399−6404.

(52) Fourmond, V.; Infossi, P.; Giudici-Orticoni, M.-T.; Bertrand, P.; Léger, C. *J. Am. Chem. Soc.* **2010**, *132*, 4848−4857.

(53) Baffert, C.; Demuez, M.; Cournac, L.; Burlat, B.; Guigliarelli, B.; Soucaille, P.; Bertrand, P.; Girbal, L.; Léger, C. *Angew. Chem., Int. Ed.* **2008**, *47*, 2052−2055.
(54) Baffert, C.; et al. *J. Am. Chem. Soc.* **2011**, *133*, 2096−2099.
(55) Sybirna, K.; Antoine, T.; Lindberg, P.; Fourmond, V.; Rousset, M.; Méjean, V.; Bottin, H. *Biomed Central Biotechnol.* **2008**, *8*, 73.
(56) Girbal, L.; von Abendroth, G.; Winkler, M.; Benton, P. M. C.; Meynial-Salles, I.; Croux, C.; Peters, J. W.; Happe, T.; Soucaille, P. *Appl. Environ. Microbiol.* **2005**, *71*, 2777−2781.
(57) Rudiger, O.; Abad, J. M.; Hatchikian, E. C.; Fernandez, V. M.; de Lacey, A. L. *J. Am. Chem. Soc.* **2005**, *127*, 16008−16009.
(58) Fourmond, V.; Hoke, K.; Heering, H. A.; Baffert, C.; Leroux, F.; Bertrand, P.; Léger, C. *Bioelectrochemistry* **2009**, *76*, 141−147.